Regular Article

blood

IMMUNOBIOLOGY

Alveolar macrophage development in mice requires L-plastin for cellular localization in alveoli

Elizabeth M. Todd,[1] Julie Y. Zhou,[1] Taylor P. Szasz,[1] Lauren E. Deady,[1] June A. D'Angelo,[2] Matthew D. Cheung,[3] Alfred H. J. Kim,[3] and Sharon Celeste Morley[1,2]

[1]Division of Infectious Diseases, Department of Pediatrics, [2]Division of Immunobiology, Department of Pathology and Immunology, and [3]Division of Rehumatology, Department of Internal Medicine, Washington University School of Medicine, St. Louis, MO

Key Points

- A key transition from the prealveolar macrophage precursor to mature alveolar macrophage is impaired in neonatal mice lacking LPL.
- Genetic impairment of neonatal alveolar macrophage development associates with impaired clearance of a pulmonary pathogen in adult animals.

Alveolar macrophages are lung-resident sentinel cells that develop perinatally and protect against pulmonary infection. Molecular mechanisms controlling alveolar macrophage generation have not been fully defined. Here, we show that the actin-bundling protein L-plastin (LPL) is required for the perinatal development of alveolar macrophages. Mice expressing a conditional allele of LPL (CD11c.Cre^{pos}-LPL$^{fl/fl}$) exhibited significant reductions in alveolar macrophages and failed to effectively clear pulmonary pneumococcal infection, showing that immunodeficiency results from reduced alveolar macrophage numbers. We next identified the phase of alveolar macrophage development requiring LPL. In mice, fetal monocytes arrive in the lungs during a late fetal stage, maturing to alveolar macrophages through a prealveolar macrophage intermediate. LPL was required for the transition from prealveolar macrophages to mature alveolar macrophages. The transition from prealveolar macrophage to alveolar macrophage requires the upregulation of the transcription factor peroxisome proliferator-activated receptor-γ (PPAR-γ), which is induced by exposure to granulocyte-macrophage colony-stimulating factor (GM-CSF). Despite abundant lung GM-CSF and intact GM-CSF receptor signaling, PPAR-γ was not sufficiently upregulated in developing alveolar macrophages in LPL$^{-/-}$ pups, suggesting that precursor cells were not correctly localized to the alveoli, where GM-CSF is produced. We found that LPL supports 2 actin-based processes essential for correct localization of alveolar macrophage precursors: (1) transmigration into the alveoli, and (2) engraftment in the alveoli. We thus identify a molecular pathway governing neonatal alveolar macrophage development and show that genetic disruption of alveolar macrophage development results in immunodeficiency. (*Blood*. 2016;128(24):2785-2796)

Introduction

Alveolar macrophages are the first responders of the pulmonary innate immune system,[1-4] protecting the host through elimination of inhaled pathogens.[5,6] Alveolar macrophages represent a distinct lineage of tissue-resident macrophages that mature during neonatal development.[7-9] During fetal development, monocytes migrate through the bloodstream to seed the embryonic lungs and subsequently upregulate CD11c and SiglecF, which identify them as mature alveolar macrophages.[10,11] Alveolar macrophage development requires the growth factor granulocyte-macrophage colony-stimulating factor (GM-CSF), which drives upregulation of the essential transcription factor peroxisome proliferator-activated receptor-γ (PPAR-γ).[8] Alveolar epithelial cells produce GM-CSF,[12] and localization to the alveolar microenvironment is required for precursors to differentiate into alveolar macrophages.[13] Under homeostatic conditions, alveolar macrophages self-renew throughout the lifespan to maintain a full complement, without repopulating from circulating blood monocytes. Despite the importance of establishing a normal complement of alveolar macrophages, key factors that regulate the timing and localization of alveolar macrophage precursors during neonatal development are incompletely described.

Here, we used mice with conditional or germ line deficiency in the actin-bundling protein L-plastin (LPL) to mechanistically probe the neonatal development of alveolar macrophages. LPL, a member of the α-actinin family, is expressed in hematopoietic cells.[14] The roles of LPL in immune cell development and function vary with cell lineage. In neutrophils, LPL is dispensable for migration, adhesion, and spreading, but required for adhesion-mediated signaling to the oxidative burst.[15] In contrast, LPL is essential for normal lymphocyte motility and trafficking.[16-20] In macrophages, LPL colocalizes with actin-supported structures and is concentrated in podosomes, which are integrin-anchored, actin-based complexes that support motility and adhesion.[21,22]

Building on our prior observation of reduced alveolar macrophage numbers in LPL$^{-/-}$ mice,[23] we now use these and newly generated CD11c.Cre^{pos}-LPL$^{fl/fl}$ mice to illuminate mechanisms of alveolar macrophage development. Specifically, we identified the key transition from prealveolar macrophage to the mature alveolar macrophage as

Submitted 18 March 2016; accepted 13 September 2016. Prepublished online as *Blood* First Edition paper, 6 October 2016; DOI 10.1182/blood-2016-03-705962.

The online version of this article contains a data supplement.

There is an Inside *Blood* Commentary on this article in this issue.

The publication costs of this article were defrayed in part by page charge payment. Therefore, and solely to indicate this fact, this article is hereby marked "advertisement" in accordance with 18 USC section 1734.

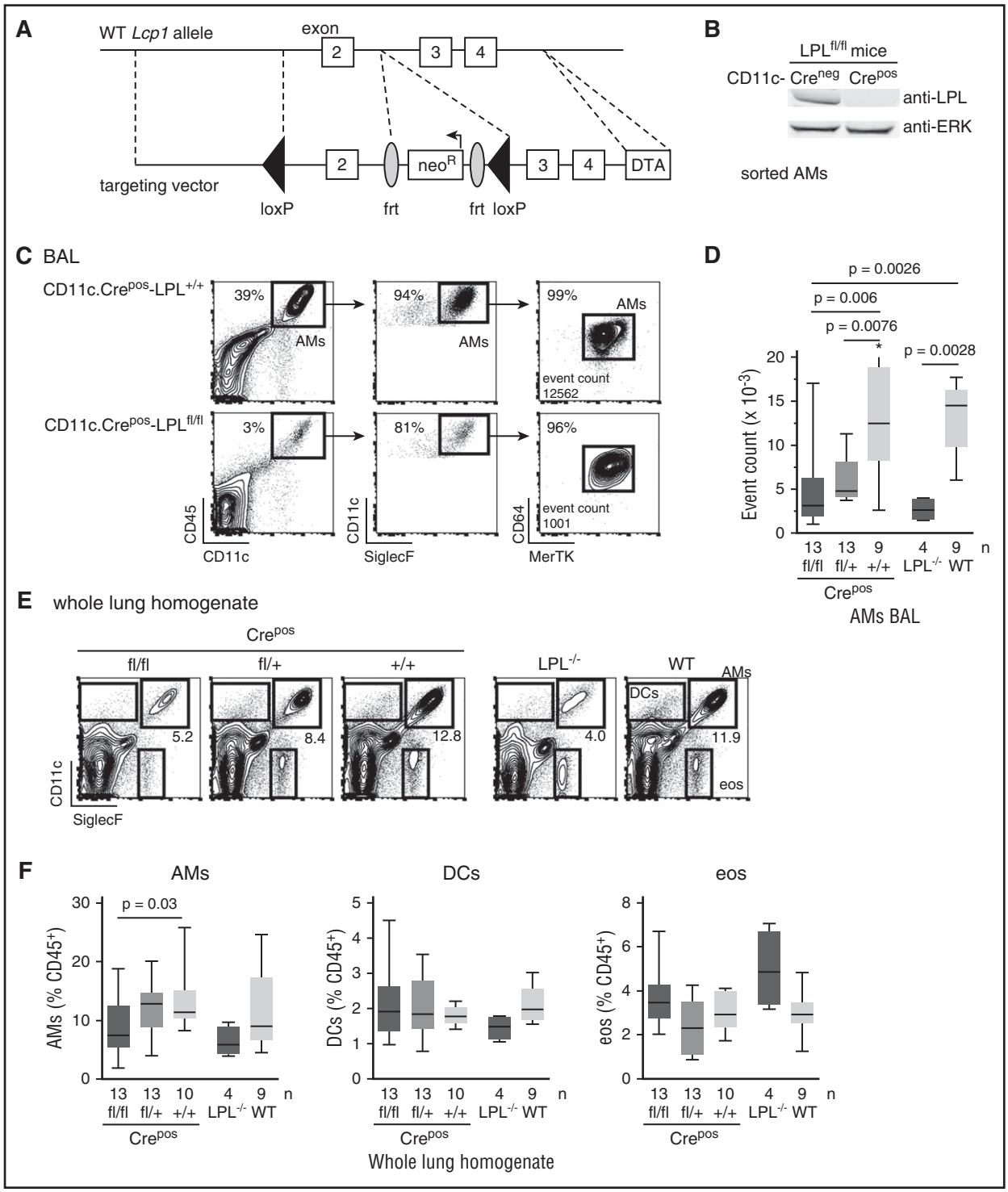

Figure 1. Reduced alveolar macrophages in CD11c.Cre^{pos} -LPL$^{fl/fl}$ and CD11.Cre^{+} -LPL$^{fl/+}$ mice. (A) Vector design for generation of conditional allele of LPL, encoded by gene *Lcp1*. A conditional allele was generated by flanking exon 2 of the gene encoding LPL, *Lcp1*, with *loxP* sequences. Exon 2 includes the ATG start site and was targeted in the generation of the LPL$^{-/-}$ mice, in which expression of LPL is deleted in all cells.[15] (B) Confirmation of deletion of LPL from CD11c^{+} alveolar macrophages sorted from adult CD11c.Cre^{pos}-LPL$^{fl/fl}$ mice, with alveolar macrophages derived from CD11c.Cre^{neg}-LPL$^{fl/fl}$ mice shown as control. (C) Representative flow cytometry of CD45^{+} singlets from the BAL fluid from mice of indicated genotypes. Alveolar macrophages identified as CD11c^{+}SiglecF^{+} cells, confirmed as macrophages by the expression of the pan-macrophage markers CD64 and MerTK. Percentage of alveolar macrophages shown in upper right corners of flow plots and event count of cells identified as alveolar macrophages given in last panels. (D) Quantification of number of alveolar macrophages in recovered BAL fluid. Data from 4 independent experiments; n given below graphs. *One outlier value of 89 070 not shown on graph but included in statistical analysis. Exclusion of this outlier does not alter the statistical significance of differences between indicated groups. (E) Representative flow cytometry of whole lung homogenates from mice of the indicated genotypes. (F) Percentage of CD45^{+} cells that were alveolar macrophages (AMs), dendritic cells (DCs), or eosinophils (eos) obtained from whole lung homogenates from mice of indicated genotypes.

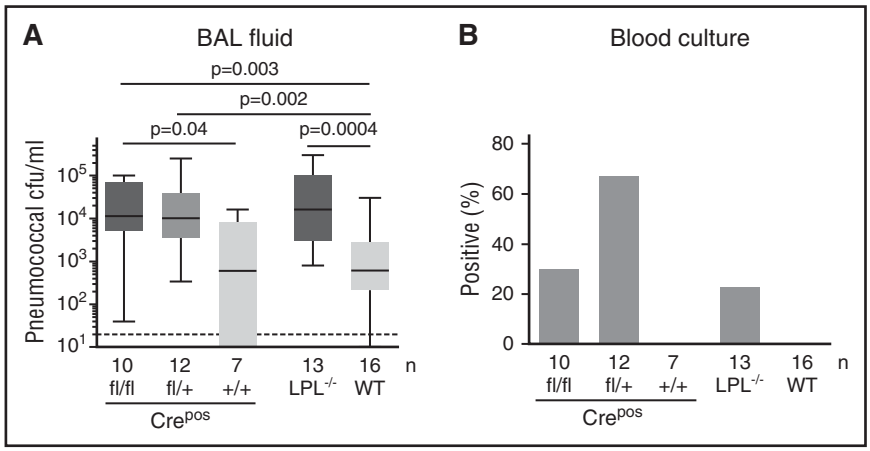

Figure 2. Impaired pneumococcal clearance and increased pneumococcal dissemination in CD11c.Cre^{pos} -LPL$^{fl/fl}$ and CD11c.Cre^{pos} -LPL$^{fl/+}$ mice. (A) Mice of indicated genotypes were challenged via intratracheal injection of 5×10^4 colony-forming units (cfu) of *S pneumoniae* serotype 3. After 24 hours, bacterial colony-forming units in harvested BAL fluid were determined by serial dilution. Number of mice shown along the x-axis; data combined from at least 3 independent experiments. (B) Percentage of mice with positive blood cultures following pulmonary pneumococcal infection.

LPL dependent. This transition failed in LPL$^{-/-}$ pups due to impaired upregulation of the essential transcription factor PPAR-γ in macrophage precursors, despite abundant GM-CSF in whole lung and intact in vitro GM-CSF receptor (GM-CSFR) signaling, suggesting restricted exposure of these precursors to alveolar GM-CSF in vivo. We subsequently found that LPL supported 2 processes critical to localizing precursor cells to the alveolar microenvironment. First, LPL-deficient monocytes were unable to traffic into the alveolar space; second, intranasally transferred LPL-deficient fetal monocytes or mature alveolar macrophages were impaired in engrafting into alveoli. Thus, we identify LPL as a novel regulator of normal alveolar macrophage development, as it enables localization of precursor cells to the alveolar microenvironment. Furthermore, cell-specific deficiency of LPL in alveolar macrophages increases susceptibility to pulmonary pneumococcal infection, exemplifying that disruption in neonatal alveolar macrophage generation imparts immunodeficiency.

Materials and methods

For details of procedures and sources of reagents, please see supplemental Methods, available on the *Blood* Web site.

Mice

LPL$^{-/-}$, CD11c.Cre^{pos}, and CD11c.YFP^{+} mice have been described.[15,17,24] Mice expressing a conditional allele of LPL (LPL$^{fl/fl}$ mice) were generated through the Hope Center Transgenic Vectors Core Facility (Washington University School of Medicine [WUSM], St. Louis, MO) and backcrossed to the C57Bl/6 background. Mice were cohoused in specific-pathogen-free barrier animal facilities, and all animal experiments were approved by the WUSM Animal Studies Committee.

Cell isolation and media

Bronchoalveolar lavage (BAL) was performed as described,[23] and cells were quantified by flow cytometry. Lungs and spleens were homogenized using 2.5 mg/mL Collagenase D in Hanks balanced salt solution + 3% fetal calf serum.[23,25] Alveolar macrophages were cultured in D10 (Dulbecco's modified Eagle medium supplemented with10% fetal calf serum). Cells deprived of serum prior to stimulation were incubated in serum-free D10 with 2% bovine serum albumin.

Flow cytometry

Commercial antibodies (clones, fluorophores, and sources) are listed in the supplemental Methods. Cells were acquired either on the BD Biosciences LSR Fortessa or with a BD FACScan flow cytometer with DxP multicolor upgrades by Cytek Development Inc (Woodland Park, NJ) and analyzed using FlowJo software (FlowJo, Ashland, OR). Cells were sorted using a BD FACSAria Fusion.

Infection

Mice were challenged intratracheally with 5×10^4 colony-forming units per animal of *Streptococcus pneumoniae* (ATCC 6303; serotype 3) in 20 μL Dulbecco's phosphate-buffered saline as previously described.[23] Mice were euthanized 24 hours after challenge, and blood and BAL fluid were obtained for culture.

Immunoblot

Immunoblots were performed as described.[18] Membranes were probed with either anti-LPL (provided by Eric J. Brown, Genentech) or with anti-PPAR-γ (clone C26H12; Cell Signaling Technology, Danvers, MA). For comparison across multiple experiments, PPAR-γ levels were normalized to the loading control (actin expression) of each sample and then to the expression of PPAR-γ in alveolar macrophages from neonatal wild-type (WT) mice in each experiment.

GM-CSF assay

Lysates of whole lung homogenates were prepared as described,[10] and GM-CSF was quantified using the Mouse GM-CSF enzyme-linked immunosorbent assay Ready-SET-Go! kit.

In vitro GM-CSF stimulation of cells

Rested cells were incubated in D10 ± GM-CSF (20 ng/mL) for 15 minutes (for induction of phosphorylated STAT5 [phospho-STAT5]) or overnight (for induction of PPAR-γ). After incubation with fluorescently labeled monoclonal antibody (mAb) to visualize surface markers, cells were fixed, and intracellular flow cytometry for phospho-STAT5 or PPAR-γ was performed.

Monocyte migration

In vitro Transwell assay. Monocytes ($5\text{-}7 \times 10^5$) isolated from bone marrow (Miltenyi Biotec) were incubated in medium (RPMI + 2% bovine serum albumin, 1 mM *N*-2-hydroxyethylpiperazine-*N*′-2-ethanesulfonic acid) in the upper chamber of Transwell inserts (3-μM pore) with CCL2 (10 ng/mL) in the lower chamber. Transmigrated monocytes were enumerated following a 90-minute incubation. The percentage of cells transmigrated was normalized to the maximum migration of WT cells (set at 100%) in each experiment.

In vivo alveolar trafficking. Either 50 μg CCL2 or phosphate-buffered saline (PBS; 20 μL) was injected intratracheally into anesthetized mice. After 20 to 24 hours, mice were euthanized, and monocytes in BAL were enumerated.

Competitive in vivo trafficking. Monocytes isolated from bone marrow (adult WT or LPL$^{-/-}$ mice) were mixed in a 1:1 ratio and transferred retro-orbitally into congenically marked postnatal day 1 to

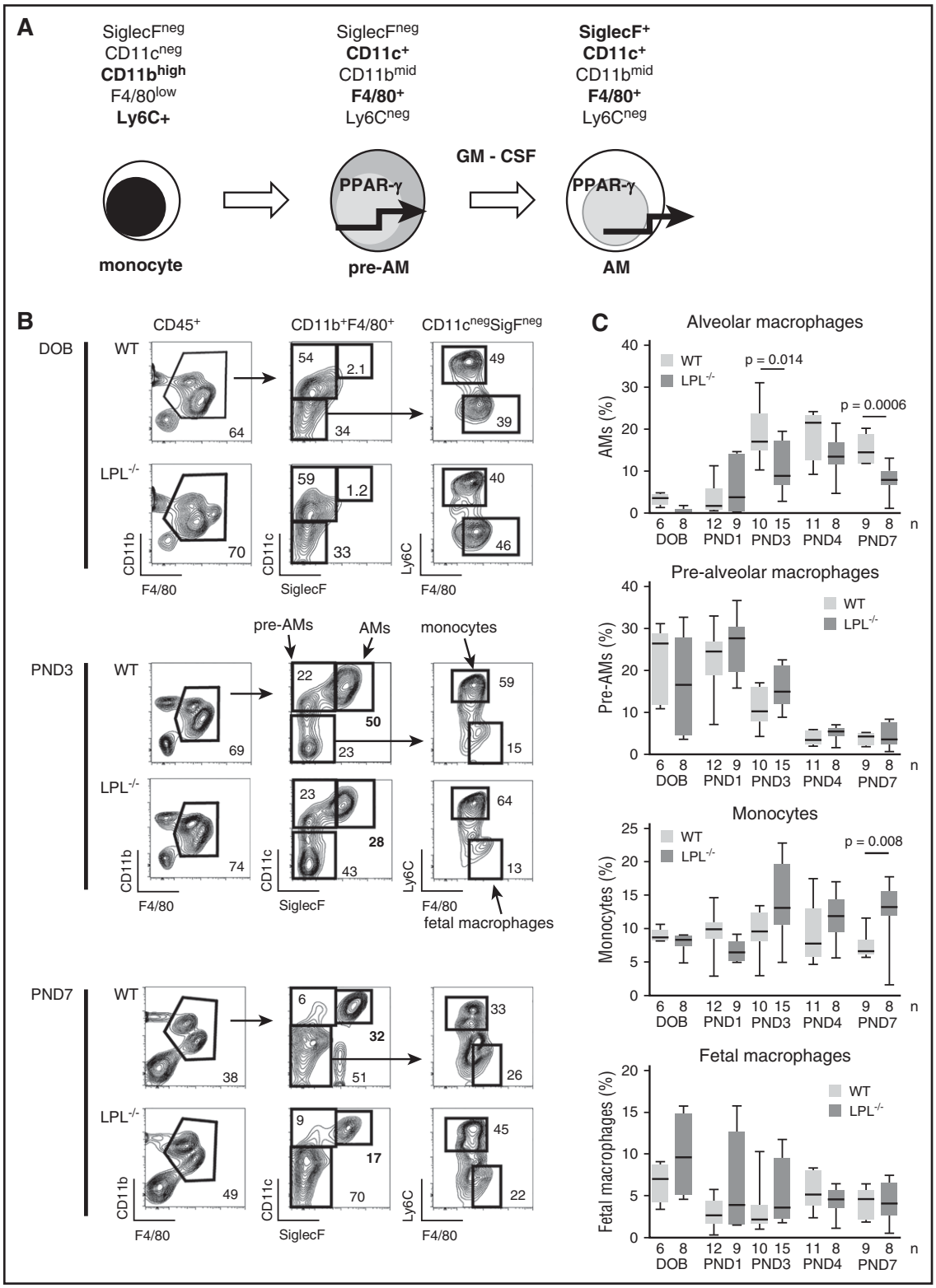

Figure 3. Transition from prealveolar macrophage intermediate to mature alveolar macrophage requires LPL. (A) During embryogenesis, fetal macrophages (not shown) derived from yolk-sac precursors are present in lung tissue. Around embryonic day 16, fetal monocytes migrate from the fetal liver to seed the lungs, presumably via the bloodstream.[10,11] During the final days of fetal development, these monocytes downregulate Ly6C and upregulate CD11c, leading to their designation as prealveolar macrophages. Following birth, prealveolar macrophages upregulate SiglecF and are then identified as mature alveolar macrophages, which appear in the alveolar space around PND1.[10] (B) Representative flow cytometry demonstrating gating scheme to identify fetal macrophages, fetal monocytes, prealveolar macrophages, and mature alveolar macrophages. Whole lung homogenates from WT or LPL$^{-/-}$ neonatal mice at indicated ages are shown. Percentages of each gate are given within each flow plot. Flow cytometric gates for each experiment were established using samples obtained from contemporaneous adult WT control animals (supplemental Figure 3A). (C) Quantification of percentage of CD45^{+} cells that were mature alveolar macrophages, prealveolar macrophages, fetal monocytes, or fetal macrophages from whole lung homogenates isolated from WT or LPL$^{-/-}$ pups. Age indicated as DOB, PND. Data for each age combined from at least 2 independent experiments; n of each sample given on the x-axis.

2 (PND1-2) WT pups. Pups were given CCL2 (5 μg) intranasally, and percentages of lung monocytes derived from donors were determined by flow cytometric analysis the next day. Data were presented as the ratio of WT-derived monocytes to $LPL^{-/-}$-derived monocytes. Input ratio was used as control, as acquiring blood for analysis from neonatal pups was not possible.

Clearing of lung tissue and 2-photon microscopy

PND7 CD11c.YFP-WT and CD11c.YFP-$LPL^{-/-}$ pups were euthanized, and lungs were perfused with PBS (30 mL) and then with 4% paraformaldehyde (Sigma; 30 mL). Lungs were removed and fixed overnight in 4% paraformaldehyde prior to clearing as previously described.[26] Cleared lungs were mounted and viewed using a custom-built 2-photon microscope (2PM) available in the WUSM In Vivo Imaging Core. Autofluorescence of lung tissue delineated alveoli. Image stacks were converted to 3-dimensional reconstructions using Imaris software (Bitplane, Zurich, Switzerland). A blinded observer manually counted round YFP^+ cells that were present either entirely within the alveoli ("alveolar localization") vs within the parenchyma.

Monocyte and alveolar macrophage engraftment

Fetal monocytes (>95% pure) were acquired via cell sorting of whole lung homogenates from congenically marked DOB-PND2 WT and $LPL^{-/-}$ pups. Mixed monocytes were transferred intranasally into congenically marked WT DOB-PND1 pups. One week later, whole lung homogenates from recipient pups were analyzed for donor origin of monocytes, prealveolar macrophages, and alveolar macrophages.

Alveolar macrophages were acquired from Percoll gradient isolation of cells from BAL of adult congenically marked WT and $LPL^{-/-}$ mice. Mixed alveolar macrophages (input $LPL^{-/-}$:WT ratio of 2:1) were transferred intranasally into congenically marked PND1 pups. Whole lung homogenates of recipient pups were prepared 24 hours and ≥72 hours after transfer and analyzed for proportions of donor WT and $LPL^{-/-}$ alveolar macrophages.

Confocal imaging

Alveolar macrophages stimulated with D10 (30 minutes) were fixed with 4% paraformaldehyde, permeabilized, and stained with either anti-LPL or anti-vinculin mAb followed by anti-mouse antibody conjugated to DyLight594. F-actin was stained with phalloidin-AlexaFluor 488. Samples were imaged using the Olympus FluoView FV1000 upright confocal microscope fitted with ×60 oil objective. Images were obtained using synchronized scanning with a multiline argon laser (457 nm, 488 nm, and 514 nm) and 635-nm diode laser on FV10-ASW 3.0 software. Percentage of cells with podosomes was determined by manual counting of images by a blinded observer.

Data analysis and statistics

Data were analyzed and graphed using Prism (GraphPad Software, Inc, La Jolla, CA). Box-and-whiskers plots show boxes representing the 25th and 75th percentiles of data, line at median, and whiskers showing minimum to maximum values. *P* values were determined using unpaired, 2-tailed Mann-Whitney *U* tests unless otherwise indicated.

Results

Cell-intrinsic requirement for LPL in alveolar macrophage development

The cell-intrinsic requirement for LPL in generating normal numbers of alveolar macrophages was established by analyzing newly generated $CD11c.Cre^{pos}$-$LPL^{fl/fl}$ mice (Figure 1A-B). We selected $CD11c.Cre^{pos}$ mice because they were previously used to show the cell-intrinsic requirement for PPAR-γ in alveolar macrophage development.[8] We confirmed that CD11c-driven Cre expression abrogated expression of LPL in alveolar macrophages from $CD11c.Cre^{pos}$-$LPL^{fl/fl}$ mice (Figure 1B). Analysis of BAL fluid demonstrated a 75% reduction of mature alveolar macrophages in $CD11c.Cre^{pos}$-$LPL^{fl/fl}$ mice, as compared with that of $CD11c.Cre^{pos}$-$LPL^{+/+}$ mice (Figure 1C-D). The conditional allele itself did not disrupt LPL expression or alveolar macrophage numbers in $CD11c.Cre^{neg}$-$LPL^{fl/fl}$ mice (Figure 1B; supplemental Figure 1). Whole lung homogenates from adult $CD11c.Cre^{pos}$-$LPL^{fl/fl}$ mice also revealed reductions in mature alveolar macrophages (Figure 1E-F). The decrease in numbers of alveolar macrophages in BAL fluid and whole lung homogenates of $CD11c.Cre^{pos}$-$LPL^{fl/fl}$ mice was similar to that of $LPL^{-/-}$ mice (Figure 1C-F; supplemental Figure 2A-B). Furthermore, mice haploinsufficient for LPL in $CD11c^+$ cells ($CD11c.Cre^{pos}$-$LPL^{fl/+}$ mice) also revealed fewer alveolar macrophages recovered from BAL fluid (Figure 1D). LPL is thus required in a cell-intrinsic manner for the generation of normal alveolar macrophage numbers.

We did not find reductions in pulmonary dendritic cells or eosinophils in $CD11.Cre^{pos}$-$LPL^{fl/fl}$ or $LPL^{-/-}$ mice (Figure 1E-F; supplemental Figure 1B). Analysis of WT and $LPL^{-/-}$ mice revealed no reductions in splenic macrophages or peripheral blood monocytes (supplemental Figure 2C-D). Thus, other innate cells localize to the lungs in $LPL^{-/-}$ mice, and not all resident macrophage populations require LPL during development.

Cell-intrinsic requirement for LPL in alveolar macrophages in preventing dissemination of pulmonary pneumococcal infection

The function of alveolar macrophages in controlling pulmonary pneumococcal challenge is unclear.[5,6,27] $LPL^{-/-}$ mice, in which all hematopoietic cells lack LPL, exhibited impaired pneumococcal clearance and increased susceptibility to infection.[23] To distinguish a cell-intrinsic requirement for LPL in alveolar macrophages from potential requirements in other immune cells (eg, neutrophils) during acute bacterial pneumonia, we assessed bacterial clearance and dissemination in $CD11c.Cre^{pos}$-$LPL^{fl/fl}$, $CD11c.Cre^{pos}$-$LPL^{fl/+}$, $CD11c.Cre^{pos}$-$LPL^{+/+}$, and control WT and $LPL^{-/-}$ mice following intratracheal instillation of *S pneumoniae*. $CD11c.Cre^{pos}$-$LPL^{fl/fl}$ and $CD11c.Cre^{pos}$-$LPL^{fl/+}$ mice exhibited significantly higher pneumococcal burden in BAL fluid 24 hours after challenge, equivalent to the impaired clearance found in $LPL^{-/-}$ mice (Figure 2A). Furthermore, dissemination of pneumococci to the bloodstream within 24 hours of infection occurred exclusively in $CD11c.Cre^{pos}$-$LPL^{fl/fl}$, $CD11c.Cre^{pos}$-$LPL^{fl/+}$, and $LPL^{-/-}$ mice (Figure 2B). Impaired clearance and increased dissemination directly correlated with the number of alveolar macrophages recovered from the BAL of $CD11c.Cre^{pos}$-$LPL^{fl/fl}$ and $CD11c.Cre^{pos}$-$LPL^{fl/+}$ mice (Figure 1D), indicating a key role for alveolar macrophages in pathogen elimination and in containing pneumococcal infection to the lung.

LPL is required during neonatal development as prealveolar macrophages transition to mature alveolar macrophages

Having established a cell-intrinsic requirement for LPL in alveolar macrophage generation and host defense, we next evaluated the mechanism by which LPL supports alveolar macrophage production (Figure 3). Alveolar macrophages develop in neonatal mice in a stepwise program (Figure 3A).[8,10,11] Alveolar macrophage numbers were reduced in $CD11c.Cre^{pos}$-$LPL^{fl/fl}$ mice, suggesting a requirement for LPL during or after the prealveolar macrophage phase when CD11c is first expressed. To define the developmental phase that requires LPL, we analyzed

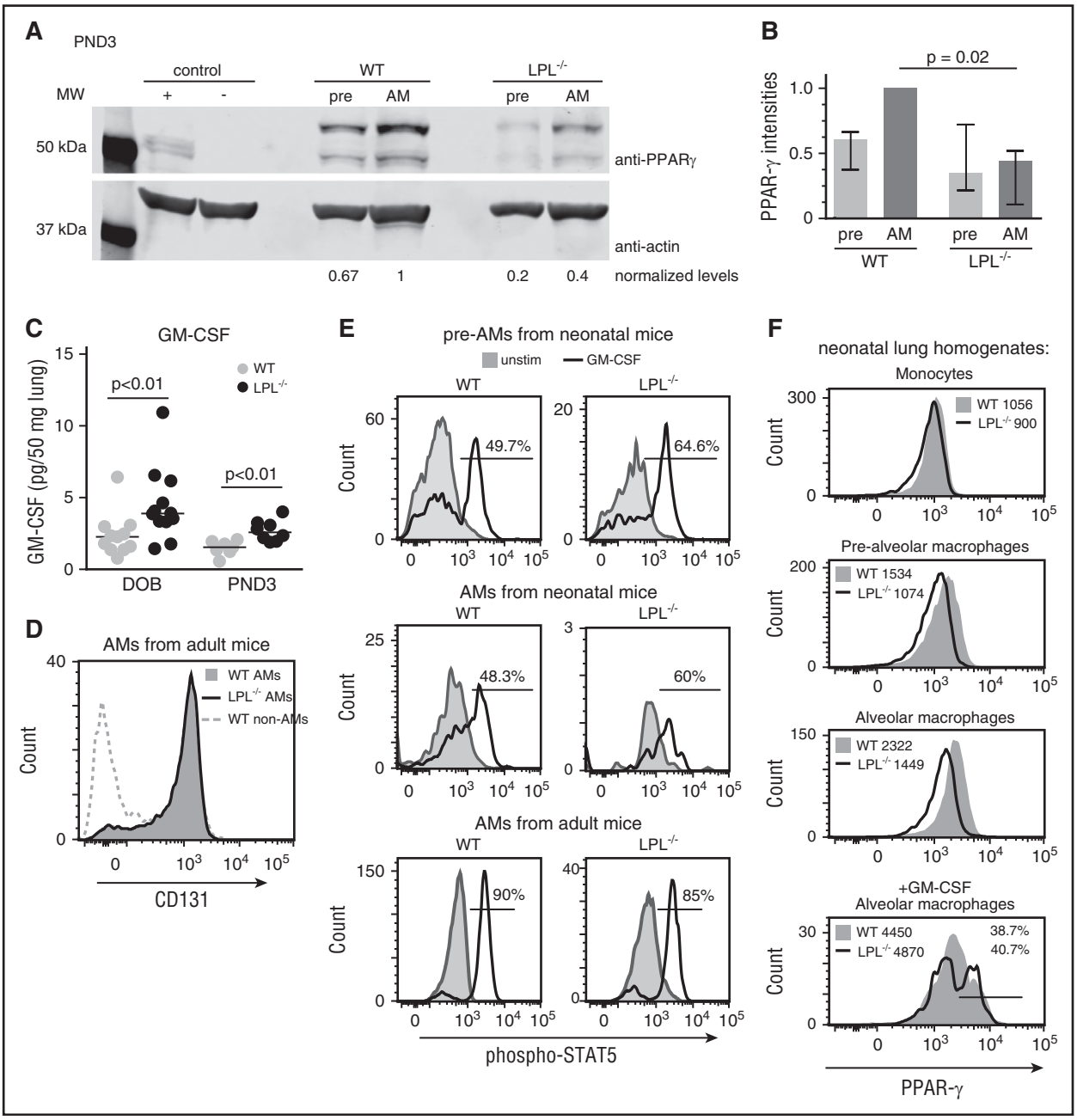

Figure 4. Developing alveolar macrophages in LPL$^{-/-}$ pups do not upregulate PPAR-γ despite abundant GM-CSF. (A) Representative immunoblot of PPAR-γ from prealveolar macrophages and alveolar macrophages sorted from whole lung homogenates of WT and LPL$^{-/-}$ neonatal (PND3) pups. Both PPAR-γ1 and PPAR-γ2 were detected in prealveolar macrophages and alveolar macrophages, although only PPAR-γ1 is found in the activated peritoneal macrophages used as a positive control. Positive control contained lysate from thioglycollate-elicited peritoneal macrophages, and the negative control contained lysate from thioglycollate-elicited peritoneal macrophages from PPAR-γ-deficient animals. Immunoblot of actin used as loading control. Density of PPAR-γ band normalized first to actin, then to WT alveolar macrophage sample, set to "1." (B) PPAR-γ levels (normalized) from 4 independent experiments. Bar shows median of 4 values with interquartile range. (C) GM-CSF concentrations, measured by enzyme-linked immunosorbent assay, from whole lung homogenates from WT (gray symbols) or LPL$^{-/-}$ (black symbols) neonatal pups. Data normalized to lung weight obtained prior to lysis. Each symbol represents data from 1 animal, line at median. Data from 3 independent experiments combined. (D) Flow cytometric analysis of CD131 on alveolar macrophages from BAL fluid from adult WT (filled gray histogram) and LPL$^{-/-}$ (solid line) mice. Cells that do not express CD131 shown as negative control (dotted gray line). Representative of at least 3 independent experiments. (E) Flow cytometric analysis of phospho-STAT5 in cells incubated for 15 minutes with (solid line) or without (filled gray histogram) GM-CSF. Prealveolar macrophages and alveolar macrophages from whole lung homogenates from WT and LPL$^{-/-}$ neonatal pups (PND1-2) and in alveolar macrophages from BAL fluid of adult WT and LPL$^{-/-}$ mice, defined by flow cytometric analysis as in Figure 3. Few fully mature alveolar macrophages were present in neonatal WT and LPL$^{-/-}$ pups. Percentage of cells positive for phospho-STAT5 given in each histogram. Representative of 2 independent experiments. (F) Intracellular flow cytometric analysis of PPAR-γ expression in cells from whole lung homogenates of WT and LPL$^{-/-}$ neonatal pups (PND1-3), with cell types defined as in supplemental Figure 3C. Median fluorescence intensity of each histogram is given. In lowest panel, cells were incubated overnight in vitro with GM-CSF (20 ng/mL); percentage and median fluorescence intensity of cells with upregulated PPAR- γ are given. Representative of 2 independent experiments. MW, molecular weight.

neonatal development in LPL$^{-/-}$ mice (as excision of LPL in CD11c. Cre^{pos}-LPL$^{fl/fl}$ mice would not occur until Cre was expressed in prealveolar macrophages, precluding analysis of earlier precursors).

We identified fetal macrophages, fetal monocytes, prealveolar macrophages, and mature alveolar macrophages of whole lung homogenates from WT and LPL$^{-/-}$ neonatal pups as previously

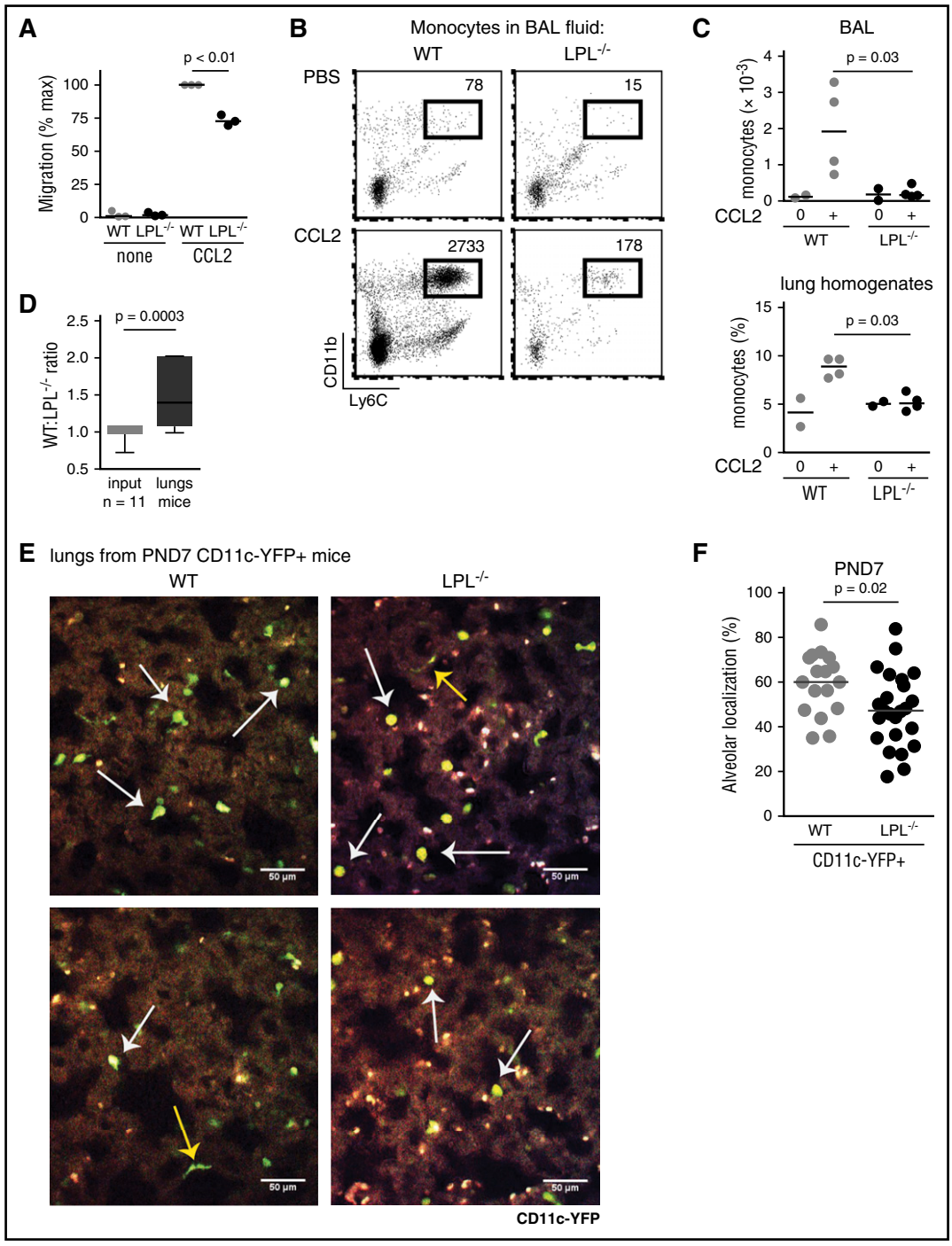

Figure 5. Monocyte trafficking into alveoli requires LPL. (A) Monocytes isolated from the bone marrow of WT (light gray circles) and LPL$^{-/-}$ (black circles) mice were allowed to migrate across Transwell inserts for 90 minutes. The percentage of migrated cells was normalized to the maximum migration of WT monocytes stimulated with CCL2 (10 ng/mL) within each experiment. Averages from duplicate samples from 3 independent experiments shown; $P < .01$ by Student t test. (B) Representative flow cytometry of BAL fluid harvested 24 hours after intratracheal CCL2 challenge of adult WT and LPL$^{-/-}$ mice. Neutrophils and alveolar macrophages excluded using Ly6G and SiglecF, respectively. Monocytes identified as CD45^{+}CD11b^{+}Ly6C^{+} cells. Total number of cells in BAL fluid shown in the upper right corner; the entire BAL sample was acquired to enumerate cells. (C) Quantification of total number of monocytes recovered from BAL fluid and percentages of monocytes in whole lung homogenates from adult WT (gray circles) or LPL$^{-/-}$ (black circles) mice challenged with intratracheal injection of CCL2 (or PBS control). Each symbol represents data from 1 animal; data from 2 independent experiments. (D) Ratio of WT to LPL$^{-/-}$ monocytes isolated from adult animals, mixed and cotransferred via retro-orbital injection into WT neonatal mice and recovered 1 day following CCL2 intranasal challenge. Input ratio is used as the control. Data combined from 14 recipient mice in 3 independent experiments. (E) Examples of images acquired via 2PM of cleared lungs from PND7 CD11c.YFP^{+}-WT or CD11c.YFP^{+}-LPL$^{-/-}$ pups. PND7 mice were the smallest pups that could be consistently thoroughly perfused. CD11c^{+} prealveolar macrophages or alveolar macrophages were easily distinguished as round, YFP+ (green/yellow) cells (white arrows) from the thin and flat dendritic cells (yellow arrows). CD11c^{+} cells were also readily distinguished from many smaller, intensely autofluorescent bodies of unclear etiology located entirely within the lung parenchyma, which were found in lungs of both CD11c.YFP^{+}-WT and CD11c.YFP^{+}-LPL$^{-/-}$ pups and may be artifact from the clearing process. Brightness and contrast were adjusted using ImageJ for display in print. Images representative of randomly selected fields from lungs of 9 CD11c.YFP^{+}-WT and 9 CD11c.YFP^{+}-LPL$^{-/-}$ pups from 2 independent experiments. Scale bar represents 50 µM. (F) Percentage of round CD11c^{+} cells localized entirely within alveoli as determined by a blinded observer who scored Z-stacks from randomly selected fields from CD11c.YFP^{+}-WT (gray circles) and CD11c.YFP^{+}-LPL$^{-/-}$ (black circles) pups. Data combined from 2 independent experiments.

established (Figure 3B).[8,10] We found equivalent frequencies of fetal macrophages, fetal monocytes, and prealveolar macrophages in the lungs from WT and LPL$^{-/-}$ pups euthanized on the DOB. Very few mature alveolar macrophages were present in neonatal pups euthanized at DOB, as expected (Figure 3B-C). Despite equivalent frequencies of precursor cells, we consistently observed a 2-fold reduction in the percentage of mature alveolar macrophages recovered from LPL$^{-/-}$ pups at PND3, PND4, and PND7 (Figure 3C). Thus, efficient transition from prealveolar macrophages to mature alveolar macrophages required LPL.

Prealveolar macrophages in LPL$^{-/-}$ mice do not upregulate PPAR-γ despite abundant GM-CSF

The alveolar microenvironment provides cues necessary to promote alveolar macrophage differentiation from monocyte precursors.[13] GM-CSF is produced by alveolar epithelial cells and induces expression of PPAR-γ, which enables the transition from prealveolar macrophage to alveolar macrophage.[8,10,12] Because this transition was impaired in LPL$^{-/-}$ pups, we analyzed PPAR-γ expression in fetal monocytes, prealveolar macrophages, and alveolar macrophages from WT and LPL$^{-/-}$ pups. As expected, fetal monocytes from WT or LPL$^{-/-}$ pups minimally expressed PPAR-γ detectable by immunoblot (data not shown). PPAR-γ was upregulated in prealveolar macrophages compared with monocytes, and in mature alveolar macrophages as compared with prealveolar macrophages. The expression of PPAR-γ was reduced in alveolar macrophages from LPL$^{-/-}$ mice as compared with alveolar macrophages from WT mice (Figure 4A-B), consistent with impaired transition from prealveolar macrophages to alveolar macrophages.

PPAR-γ upregulation requires exposure to GM-CSF.[8] We therefore tested 5 nonexclusive possible mechanisms for reduced PPAR-γ upregulation in LPL-deficient alveolar macrophages: (1) reduced GM-CSF production; (2) reduced expression of GM-CSFR; (3) reduced signaling through GM-CSFR; (4) reduced localization of precursor cells to the alveoli, where GM-CSF is produced; and (5) reduced alveolar retention of alveolar macrophages or precursor cells.

Analysis revealed that GM-CSF concentrations were significantly elevated in lungs from LPL$^{-/-}$ pups compared with that of WT pups (Figure 4C), eliminating the first scenario. The second mechanism was also eliminated because the β chain of the GM-CSFR, CD131, was expressed equivalently on alveolar macrophages in adult WT and LPL$^{-/-}$ mice (Figure 4D). To test whether LPL was required for signaling through GM-CSFR, we evaluated both induction of STAT5 phosphorylation[28] and upregulation of PPAR-γ following exposure to GM-CSF in vitro (Figure 4E-F). We observed a similar increase in phospho-STAT5 in prealveolar and alveolar macrophages in WT and LPL$^{-/-}$ neonatal mice and in alveolar macrophages from WT and LPL$^{-/-}$ adult mice following in vitro exposure to GM-CSF (Figure 4E).

Next, we used intracellular flow cytometry to measure upregulation of PPAR-γ in cells stimulated with GM-CSF in vitro (Figure 4F). As observed by immunoblot, expression of PPAR-γ was reduced in LPL-deficient alveolar macrophages. However, alveolar macrophages from LPL$^{-/-}$ mice upregulated PPAR-γ to the same extent as did alveolar macrophages from WT mice after overnight incubation with GM-CSF (Figure 4F). Thus, we eliminated impaired GM-CSFR signaling as a possible mechanism.

Monocyte trafficking into the alveoli requires LPL

Because localization to the alveolar microenvironment is required for the acquisition of the alveolar macrophage phenotype, we evaluated a possible requirement of LPL for precursor cell migration into alveoli. We first tested the requirement for LPL in monocyte motility using a standard in vitro Transwell assay with the well-established monocyte chemokine CCL2.[29] We observed significant in vitro reduction in CCL2-mediated migration of bone marrow monocytes from LPL$^{-/-}$ mice (Figure 5A). To assess the in vivo requirement for LPL in monocyte migration into alveoli, we performed intratracheal instillation of CCL2[30] in WT and LPL$^{-/-}$ mice. CCL2 administration recruited monocytes into BAL fluid and whole lung homogenates in WT mice, whereas significantly fewer monocytes were recruited in LPL$^{-/-}$ mice (Figure 5B-C).

We confirmed a cell-intrinsic requirement for LPL in monocyte migration in a competitive in vivo assay (Figure 5D). Monocytes were isolated from the bone marrow of congenically marked WT and LPL$^{-/-}$ mice, mixed, and cotransferred IV into neonatal WT mice. These neonatal mice then underwent intranasal instillation of CCL2. Analysis revealed a significant increase in the ratio of WT:LPL$^{-/-}$ monocytes found within the lungs, compared with the ratio of WT:LPL$^{-/-}$ monocytes injected (Figure 5D). Thus, LPL is required in a cell-intrinsic manner for CCL2-directed migration of monocytes from the circulation into lung tissue.

The hypothesis that LPL supports alveolar transmigration predicts that fewer CD11c^{+} cells (representing prealveolar or alveolar macrophages) would be present in alveoli of neonatal LPL$^{-/-}$ mice. We therefore generated CD11c.YFP-LPL$^{-/-}$ mice, because alveolar macrophages can be visualized using 2PM of lung tissue from CD11c.YFP^{+} animals.[31] A blinded observer determined the percentages of round YFP^{+} cells localized entirely within alveoli in randomly selected Z-stack sections of cleared lungs harvested from PND7 CD11c.YFP-WT and CD11c.YFP-LPL$^{-/-}$ pups and viewed as 3-dimensional projections (Figure 5E; supplemental Videos 1-4). Alveolar macrophages (or prealveolar macrophages) were easily distinguished from CD11c^{+} dendritic cells on the basis of distinct morphologies: macrophages are large, round cells (Figure 5E white arrows), whereas dendritic cells are long, thin, and stellate (Figure 5E yellow arrows).[31] We compared the frequencies of round YFP^{+} cells present entirely within the alveoli of each imaged section, not absolute numbers, because the penetrance of YFP expression on CD11c^{+} alveolar macrophages varied among mice (supplemental Figure 3D). We found a decreased frequency of round YFP^{+} cells entirely within the alveoli in CD11c.YFP-LPL$^{-/-}$ pups (Figure 5F), consistent with the proposed mechanism that alveolar transmigration is impeded in the absence of LPL.

LPL required for engraftment of monocytes and alveolar macrophages into alveoli

Finally, we tested if LPL was required for retention of precursor cells and/or alveolar macrophages within alveoli. Because adoptive transfer of monocytes into the airways of recipient mice induces differentiation into alveolar macrophages,[10,32] we evaluated a requirement for LPL in monocyte engraftment by performing competitive intranasal adoptive transfers of monocytes derived from neonatal WT and LPL$^{-/-}$ pups, as previously described (Figure 6A).[10] One week after adoptive transfer of mixed donor monocytes, lungs were harvested from recipient pups and analyzed for alveolar macrophages derived from donor cells (Figure 6B). Mature alveolar macrophages derived from donor WT monocytes were readily identified (Figure 6B-C). However, we could not detect any population—monocyte, prealveolar macrophage, or alveolar macrophage—derived from the cotransferred LPL$^{-/-}$ precursors (Figure 6B-C; data not shown). Thus, there was marked impairment in the ability of monocyte precursors from LPL$^{-/-}$ neonatal donors to engraft and generate mature alveolar macrophages in recipient animals following adoptive transfer into the airways.

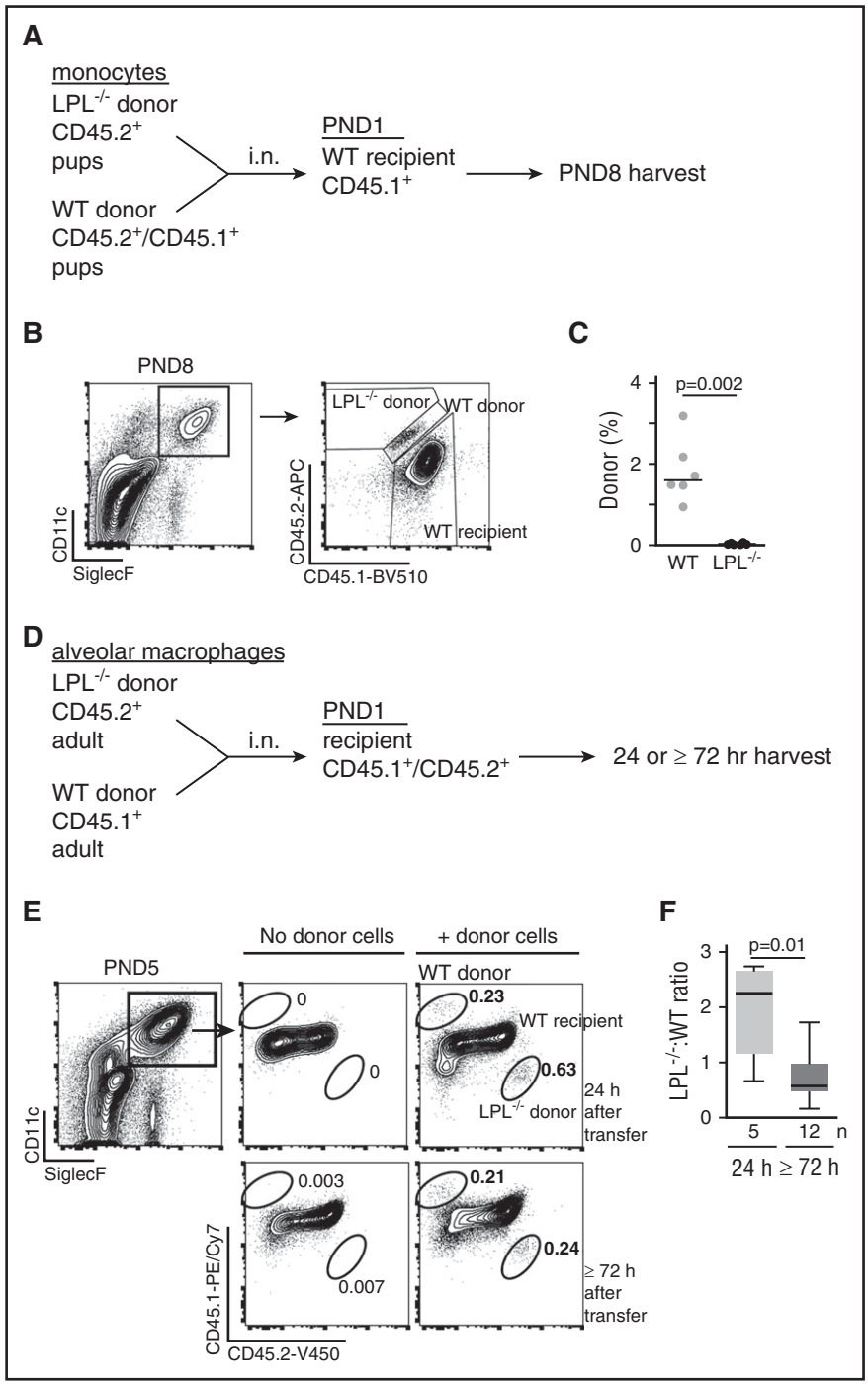

Figure 6. LPL is required for engraftment into the alveolar space. (A) Schematic of competitive transfer experiment. Fetal monocytes were sorted from the lungs of congenically marked WT (CD45.1$^+$/CD45.2$^+$) and LPL$^{-/-}$ (CD45.2$^+$) neonatal pups. Precursors were mixed in equal proportions and transferred by intranasal (i.n.) administration into congenically marked WT (CD45.1$^+$) neonatal pup recipients. Neonatal pups were employed as donors and recipients so as to evaluate engraftment and alveolar macrophage generation during the physiologically relevant developmental window. After 1 week, lungs were harvested and analyzed for alveolar macrophages derived from donor monocytes. (B) Representative flow cytometry from 1 recipient pup, demonstrating gating for mature alveolar macrophages and determination of origin. Flow cytometry plots showing controls for gating of CD45.1, CD45.2, and CD45.1/CD45.2 populations shown in supplemental Figure 2. (C) Percentage of alveolar macrophages derived from either WT (gray circles) or LPL$^{-/-}$ (black circles) donor pups. Each symbol represents data from 1 recipient animal from 2 independent experiments. (D) Schematic of competitive transfer experiment in which alveolar macrophages were isolated from BAL fluid of congenically marked adult WT and LPL$^{-/-}$ mice, mixed and coinjected intranasally into marked recipient PND1 pups. After 24 or ≥72 hours, lungs were harvested and analyzed for alveolar macrophages derived from donor mice. (E) Representative flow cytometric analysis of a recipient pup to evaluate presence of donor alveolar macrophages. As neonatal development of alveolar macrophages was actively ongoing in recipients, the proportion of transferred alveolar macrophages was low. (F) Ratios of LPL$^{-/-}$-derived:WT-derived alveolar macrophages recovered from recipient pups at the indicated times after adoptive transfer. We delivered more alveolar macrophages from LPL$^{-/-}$ mice to ensure detection of LPL$^{-/-}$-derived cells after 24 hours.

To test if alveolar macrophages required LPL for engraftment, we performed competitive adoptive transfer assays using alveolar macrophages from congenically marked adult WT and LPL$^{-/-}$ mice and neonatal recipients (Figure 6D). Flow cytometric analysis of recipient lungs 24 hours after transfer revealed that alveolar macrophages from WT and LPL$^{-/-}$ donors could be detected (Figure 6E). We deliberately delivered more alveolar macrophages from LPL$^{-/-}$ mice than WT (to ensure detection after transfer) with a median ratio of LPL$^{-/-}$-derived:WT-derived cells of ~2:1 (Figure 6F). Analysis of recipient lungs ≥72 hours after transfer revealed a significant decline in alveolar macrophages from LPL$^{-/-}$ donors (Figure 6E-F). Our data thus support the hypothesis that another mechanism by which LPL supports alveolar macrophage development is through enabling retention of cells within alveoli.

LPL is essential for podosome formation

Monocyte/macrophage migration and adhesion rely upon the formation of podosomes,[33-35] which are visualized as bright F-actin dots surrounded by integrin-associated proteins such as vinculin. LPL was previously reported to be concentrated in macrophage podosomes.[36-38] Here, imaging of fixed alveolar macrophages from WT mice revealed colocalization between F-actin and LPL, including in podosomes (Figure 7A, arrows). To determine whether LPL was required for

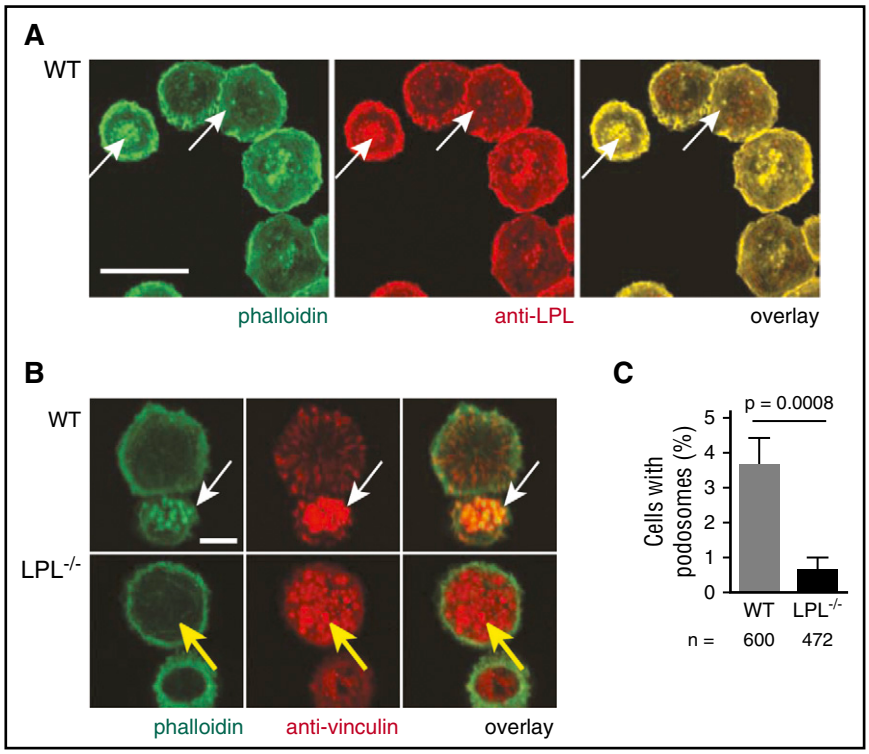

Figure 7. LPL is essential for alveolar macrophage podosome formation. (A) Alveolar macrophages from adult WT mice were applied to glass coverslips and fixed. F-actin was illuminated by staining with phalloidin-AlexaFluor 488 (green), and LPL was labeled with anti-LPL mAb followed by DyLight594 (red). LPL colocalizes with F-actin in podosomes (white arrows). Scale bar shows 20 μM. (B) Confocal image analysis demonstrating podosome formation in alveolar macrophages from adult WT animals (white arrow) with a podosome defined as an actin dot (green) surrounded by anti-vinculin staining (red). Podosomes did not form well, if at all, in alveolar macrophages from adult LPL$^{-/-}$ mice (yellow arrow). Scale bar shows 5 μM. (C) Percentage of alveolar macrophages with podosomes from adult WT (gray bar) or LPL$^{-/-}$ (black bar) mice. Data from 3 independent experiments combined; the standard errors of the mean of the proportions are shown and were calculated using the formula standard error = $\sqrt{(p^*(1 - p)/n)}$, where p represents proportion and n represents the number of samples; *P* value was determined using Fisher's exact test.

podosome formation, freshly isolated alveolar macrophages from WT or LPL$^{-/-}$ mice were examined by confocal microscopy (Figure 7B). Podosomes were defined as vinculin-encircled F-actin punctae (Figure 7B, white arrow, WT). Alveolar macrophages from LPL$^{-/-}$ mice exhibited significantly reduced podosome formation (Figure 7B-C, yellow arrow), offering a molecular explanation for impaired migration and engraftment.

Discussion

The ontogeny of alveolar macrophages is unique among macrophage lineages.[39,40] Recent work has defined a perinatal progression during which yolk sac–derived monocytes arrive in fetal lungs, progress to a prealveolar macrophage phase in the days preceding birth, and evolve as a mature alveolar macrophage phenotype following birth.[4,8,10,41] Our work illuminates 2 mechanisms by which LPL expression in neonatal precursor cells is critical for their transition to alveolar macrophages. In addition, reduced numbers of LPL-deficient alveolar macrophages recoverable from the bronchoalveolar space directly correlated with impaired pulmonary clearance and enhanced dissemination of pneumococci, showing that genetic disruption of alveolar macrophage generation results in immunodeficiency.

LPL supports podosome formation in alveolar macrophages.[34,42] Podosomes are integrin-based, complex multimolecular organelles that consist of a branched F-actin core surrounded by unbranched, bundled F-actin.[36,43-45] Podosomes enable monocyte and macrophage migration and adhesion,[34] and LPL was previously shown to be a major component of podosomes.[21,22,36,38] Podosome formation was disrupted in LPL-deficient alveolar macrophages, as measured by colocalization of actin and vinculin. Podosome disruption in alveolar macrophages was more profound than that observed in LPL-deficient peritoneal macrophages, in which vinculin and F-actin colocalization occurred efficiently,[46] indicating that this function of LPL varies with macrophage lineage.

Podosome disruption could underlie the observed migration and retention defects. First, monocyte precursors relied on LPL for normal migration into alveoli. Although LPL was previously shown to be required for normal motility in lymphocytes,[17,18,47] it was dispensable for motility in neutrophils.[15] The defect in monocyte alveolar transmigration in LPL$^{-/-}$ mice was more profound than that of monocyte trafficking into the peritoneum,[46] suggesting that different tissues present distinct environments for cellular migration.

Although precursor cells must localize to the alveoli to terminally differentiate into alveolar macrophages, it is not currently clear whether monocytes, prealveolar macrophages, or both, transmigrate perinatally to give rise to alveolar macrophages. We employed numerous techniques to further specify the histological location of precursors, but lung tissue autofluorescence, difficulty in perfusing and aerating neonatal murine lungs, and thin alveolar walls made such identification technically impracticable. Using the recently described lung-clearing technique[26] and 2PM with CD11c.YFP^{+} reporter mice, we were able to visualize whether prealveolar/alveolar macrophages were entirely within alveoli or partially embedded in parenchyma in PND7 pups. A lower frequency of CD11c-YFP^{+} cells were entirely within the alveoli in CD11c.YFP^{+}-LPL$^{-/-}$ mice, consistent with a model in which LPL promotes efficient transmigration of cells into alveoli.

Second, monocytes from LPL$^{-/-}$ mice did not engraft, and alveolar macrophages from LPL$^{-/-}$ mice were lost more quickly than those from WT donors, following intranasal transfer into alveoli. These observations suggest that LPL-supported podosomes also enable retention of precursors and alveolar macrophages within alveoli. Localization of precursors to the alveolar niche exposes them to the growth factor GM-CSF, which is secreted by alveolar epithelial cells and induces PPAR-γ.[8,10,13,39,48] GM-CSF production was significantly elevated in neonatal LPL$^{-/-}$ mice, consistent with a previously hypothesized feedback loop, centered in the alveoli, in

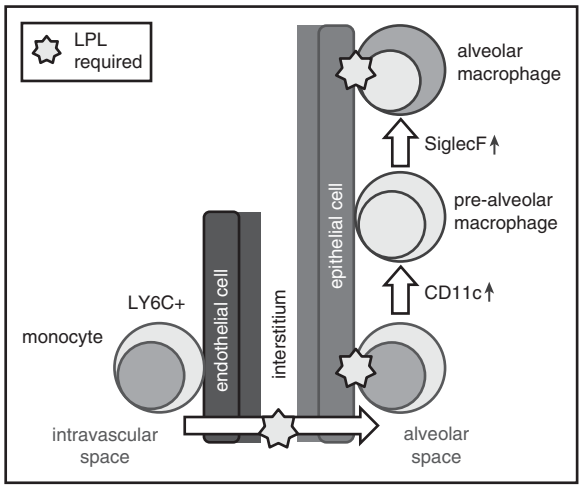

Figure 8. LPL is required for the generation of alveolar macrophages and supports transmigration of cells into alveoli and retention within the alveolar microenvironment. Our data suggest a model in which LPL is required for transmigration of alveolar macrophage precursors into the alveoli during development. Our data also show that LPL is required for engraftment of monocytes and/or mature alveolar macrophages into alveoli.

which alveolar epithelial cells sense and respond to reduced numbers of maturing alveolar macrophages by upregulating GM-CSF.[13] Reduced PPAR-γ expression in alveolar macrophages in LPL$^{-/-}$ pups, despite abundant GM-CSF and apparently intact GM-CSFR signaling, strongly suggests reduced exposure to GM-CSF, which we propose is secondary to impaired trafficking into and/or engraftment within the alveolar microenvironment (Figure 8).

Our data also highlight the narrow temporal window that exists for alveolar macrophage development. Despite a paucity of alveolar macrophages and increased GM-CSF levels, prealveolar macrophage generation terminated in LPL$^{-/-}$ mice between PND3 and PND4. These data indicate that lung factors beyond GM-CSF restrict alveolar macrophage development to the early neonatal period. Closure of this developmental window prevents LPL$^{-/-}$ pups from ultimately attaining a normal alveolar macrophage population, and as a result, these mice remain susceptible to pulmonary bacterial infection into adulthood.

Defining a defect in alveolar macrophage generation, based on reduced transmigration and/or alveolar retention of precursors, as a predisposing risk factor for pneumococcal susceptibility offers a new paradigm for exploring novel risk factors in human populations. Although antecedent viral infections, smoking, alcoholism, and advanced age have been identified as risk factors for severe pneumococcal pneumonia, many apparently otherwise healthy people are also susceptible.[49-51] Here, we demonstrate that even haploinsufficiency of an actin-bundling protein impairs alveolar macrophage generation and results in lifelong susceptibility to pulmonary pneumococcal challenge. These results hint that genetic variance in a class of cytoskeletal modulators not previously associated with immunodeficiency could influence susceptibility to pneumonia in the human population.

Acknowledgments

The authors thank Darren Kreamalmeyer for technical assistance with support of the mouse colony. The authors also thank David A. Hunstad, Anthony French, Mary Dinauer, Gerald Morris, and Paul M. Allen for critical review of the manuscript.

This work was supported by a Basil O'Connor Starter Scholar Award (S.C.M.), a Basic Research Grant from the American Lung Association (S.C.M.), a Grant-in-Aid from the American Heart Association (S.C.M.), the Children's Discovery Institute (grant MD-FR-2010-83) (S.C.M.), and the National Institutes of Health, National Institute of Allergy and Infectious Diseases (R01-AI104732) (S.C.M.). This work was supported by the Hope Center Transgenic Vectors Core at WUSM. Experimental support was also provided by the Speed Congenics Facility of the Rheumatic Diseases Core Center. Research reported in this publication was supported by the National Institutes of Health, National Institute of Arthritis and Musculoskeletal and Skin Diseases (P30-AR048335).

Authorship

Contribution: S.C.M. conceptualized the study; E.M.T., J.A.D., and S.C.M. provided the methodology; E.M.T., J.Y.Z., T.P.S., M.D.C., A.H.J.K., and L.E.D. investigated the data; S.C.M. wrote the original manuscript; E.M.T. and S.C.M. reviewed and edited the manuscript; and S.C.M. acquired funding and supervised the work.

Conflict-of-interest disclosure: The authors declare no competing financial interests.

The current affiliation for J.A.D. is Department of Molecular Microbiology and Immunology, Saint Louis University, St. Louis, MO.

ORCID profiles: S.C.M., 0000-0001-8424-0121.

Correspondence: Sharon Celeste Morley, Campus Box 8208, 660 South Euclid Ave, St. Louis, MO, 63110; e-mail: morley_c@kids.wustl.edu.

References

1. Martí-Lliteras P, Regueiro V, Morey P, et al. Nontypeable Haemophilus influenzae clearance by alveolar macrophages is impaired by exposure to cigarette smoke. *Infect Immun*. 2009;77(10):4232-4242.
2. Steinwede K, Tempelhof O, Bolte K, et al. Local delivery of GM-CSF protects mice from lethal pneumococcal pneumonia. *J Immunol*. 2011;187(10):5346-5356.
3. Schneider C, Nobs SP, Heer AK, et al. Alveolar macrophages are essential for protection from respiratory failure and associated morbidity following influenza virus infection. *PLoS Pathog*. 2014;10(4):e1004053.
4. Kopf M, Schneider C, Nobs SP. The development and function of lung-resident macrophages and dendritic cells. *Nat Immunol*. 2015;16(1):36-44.
5. Camberlein E, Cohen JM, José R, et al. Importance of bacterial replication and alveolar macrophage-independent clearance mechanisms during early lung infection with Streptococcus pneumoniae. *Infect Immun*. 2015;83(3):1181-1189.
6. Knapp S, Leemans JC, Florquin S, et al. Alveolar macrophages have a protective antiinflammatory role during murine pneumococcal pneumonia. *Am J Respir Crit Care Med*. 2003;167(2):171-179.
7. Gautier EL, Shay T, Miller J, et al; Immunological Genome Consortium. Gene-expression profiles and transcriptional regulatory pathways that underlie the identity and diversity of mouse tissue macrophages. *Nat Immunol*. 2012;13(11):1118-1128.
8. Schneider C, Nobs SP, Kurrer M, Rehrauer H, Thiele C, Kopf M. Induction of the nuclear receptor PPAR-γ by the cytokine GM-CSF is critical for the differentiation of fetal monocytes into alveolar macrophages. *Nat Immunol*. 2014;15(11):1026-1037.
9. Mass E, Ballesteros I, Farlik M, et al. Specification of tissue-resident macrophages during

organogenesis. *Science*. 2016, in press, pii: aaf4238.

10. Guilliams M, De Kleer I, Henri S, et al. Alveolar macrophages develop from fetal monocytes that differentiate into long-lived cells in the first week of life via GM-CSF. *J Exp Med*. 2013;210(10): 1977-1992.
11. Gomez Perdiguero E, Klapproth K, Schulz C, et al. Tissue-resident macrophages originate from yolk-sac-derived erythro-myeloid progenitors. *Nature*. 2015;518(7540):547-551.
12. Hashimoto D, Chow A, Noizat C, et al. Tissue-resident macrophages self-maintain locally throughout adult life with minimal contribution from circulating monocytes. *Immunity*. 2013; 38(4):792-804.
13. Suzuki T, Arumugam P, Sakagami T, et al. Pulmonary macrophage transplantation therapy. *Nature*. 2014;514(7523):450-454.
14. Morley SC. The actin-bundling protein L-plastin: a critical regulator of immune cell function. *Int J Cell Biol*. 2012;2012:935173.
15. Chen H, Mocsai A, Zhang H, et al. Role for plastin in host defense distinguishes integrin signaling from cell adhesion and spreading. *Immunity*. 2003;19(1):95-104.
16. Lin SL, Chien CW, Han CL, et al. Temporal proteomics profiling of lipid rafts in CCR6-activated T cells reveals the integration of actin cytoskeleton dynamics. *J Proteome Res*. 2010; 9(1):283-297.
17. Morley SC, Wang C, Lo WL, et al. The actin-bundling protein L-plastin dissociates CCR7 proximal signaling from CCR7-induced motility. *J Immunol*. 2010;184(7):3628-3638.
18. Todd EM, Deady LE, Morley SC. The actin-bundling protein L-plastin is essential for marginal zone B cell development. *J Immunol*. 2011; 187(6):3015-3025.
19. Freeley M, O'Dowd F, Paul T, et al. L-plastin regulates polarization and migration in chemokine-stimulated human T lymphocytes. *J Immunol*. 2012;188(12):6357-6370.
20. Dubovsky JA, Chappell DL, Harrington BK, et al. Lymphocyte cytosolic protein 1 is a chronic lymphocytic leukemia membrane-associated antigen critical to niche homing. *Blood*. 2013; 122(19):3308-3316.
21. Messier JM, Shaw LM, Chafel M, Matsudaira P, Mercurio AM. Fimbrin localized to an insoluble cytoskeletal fraction is constitutively phosphorylated on its headpiece domain in adherent macrophages. *Cell Motil Cytoskeleton*. 1993;25(3):223-233.
22. De Clercq S, Boucherie C, Vandekerckhove J, Gettemans J, Guillabert A. L-plastin nanobodies perturb matrix degradation, podosome formation, stability and lifetime in THP-1 macrophages. *PLoS One*. 2013;8(11):e78108.
23. Deady LE, Todd EM, Davis CG, et al. L-plastin is essential for alveolar macrophage production and control of pulmonary pneumococcal infection. *Infect Immun*. 2014; 82(5):1982-1993.
24. Stranges PB, Watson J, Cooper CJ, et al. Elimination of antigen-presenting cells and autoreactive T cells by Fas contributes to prevention of autoimmunity. *Immunity*. 2007; 26(5):629-641.
25. Edelson BT, Kc W, Juang R, et al. Peripheral CD103+ dendritic cells form a unified subset developmentally related to CD8alpha+ conventional dendritic cells. *J Exp Med*. 2010; 207(4):823-836.
26. Yang B, Treweek JB, Kulkarni RP, et al. Single-cell phenotyping within transparent intact tissue through whole-body clearing. *Cell*. 2014;158(4): 945-958.
27. Rosendahl A, Bergmann S, Hammerschmidt S, Goldmann O, Medina E. Lung dendritic cells facilitate extrapulmonary bacterial dissemination during pneumococcal pneumonia. *Front Cell Infect Microbiol*. 2013;3:doi:10.3389/fcimb.2013.00021.
28. Lehtonen A, Matikainen S, Miettinen M, Julkunen I. Granulocyte-macrophage colony-stimulating factor (GM-CSF)-induced STAT5 activation and target-gene expression during human monocyte/macrophage differentiation. *J Leukoc Biol*. 2002; 71(3):511-519.
29. Deshmane SL, Kremlev S, Amini S, Sawaya BE. Monocyte chemoattractant protein-1 (MCP-1): an overview. *J Interferon Cytokine Res*. 2009;29(6): 313-326.
30. Maus UA, Waelsch K, Kuziel WA, et al. Monocytes are potent facilitators of alveolar neutrophil emigration during lung inflammation: role of the CCL2-CCR2 axis. *J Immunol*. 2003; 170(6):3273-3278.
31. Westphalen K, Gusarova GA, Islam MN, et al. Sessile alveolar macrophages communicate with alveolar epithelium to modulate immunity. *Nature*. 2014;506(7489):503-506.
32. Trapnell BC, Carey BC, Uchida K, Suzuki T. Pulmonary alveolar proteinosis, a primary immunodeficiency of impaired GM-CSF stimulation of macrophages. *Curr Opin Immunol*. 2009;21(5):514-521.
33. Guiet R, Vérollet C, Lamsoul I, et al. Macrophage mesenchymal migration requires podosome stabilization by filamin A. *J Biol Chem*. 2012; 287(16):13051-13062.
34. Linder S, Wiesner C. Tools of the trade: podosomes as multipurpose organelles of monocytic cells. *Cell Mol Life Sci*. 2015;72(1): 121-135.
35. Wiesner C, Le-Cabec V, El Azzouzi K, Maridonneau-Parini I, Linder S. Podosomes in space: macrophage migration and matrix degradation in 2D and 3D settings. *Cell Adhes Migr*. 2014;8(3):179-191.
36. Evans JG, Correia I, Krasavina O, Watson N, Matsudaira P. Macrophage podosomes assemble at the leading lamella by growth and fragmentation. *J Cell Biol*. 2003;161(4): 697-705.
37. Correia I, Chu D, Chou YH, Goldman RD, Matsudaira P. Integrating the actin and vimentin cytoskeletons. adhesion-dependent formation of fimbrin-vimentin complexes in macrophages. *J Cell Biol*. 1999;146(4): 831-842.
38. Babb SG, Matsudaira P, Sato M, Correia I, Lim SS. Fimbrin in podosomes of monocyte-derived osteoclasts. *Cell Motil Cytoskeleton*. 1997;37(4): 308-325.
39. Gibbings SL, Goyal R, Desch AN, et al. Transcriptome analysis highlights the conserved difference between embryonic and postnatal-derived alveolar macrophages. *Blood*. 2015; 126(11):1357-1366.
40. Morales-Nebreda L, Misharin AV, Perlman H, Budinger GR. The heterogeneity of lung macrophages in the susceptibility to disease. *Eur Respir Rev*. 2015;24(137): 505-509.
41. Yona S, Kim KW, Wolf Y, et al. Fate mapping reveals origins and dynamics of monocytes and tissue macrophages under homeostasis [published correction appears in *Immunity*. 2013;38(5):1073-1079]. *Immunity*. 2013;38(1): 79-91.
42. Calle Y, Burns S, Thrasher AJ, Jones GE. The leukocyte podosome. *Eur J Cell Biol*. 2006;85(3-4): 151-157.
43. Murphy DA, Courtneidge SA. The 'ins' and 'outs' of podosomes and invadopodia: characteristics, formation and function. *Nat Rev Mol Cell Biol*. 2011;12(7):413-426.
44. Vicente-Manzanares M, Choi CK, Horwitz AR. Integrins in cell migration–the actin connection. *J Cell Sci*. 2009;122(Pt 2):199-206.
45. Hogg N, Patzak I, Willenbrock F. The insider's guide to leukocyte integrin signalling and function. *Nat Rev Immunol*. 2011;11(6): 416-426.
46. Zhou JY, Szasz TP, Stewart-Hutchinson PJ, et al. L-Plastin promotes podosome longevity and supports macrophage motility. *Mol Immunol*. 2016;78:79-88.
47. Todd EM, Deady LE, Morley SC. Intrinsic T- and B-cell defects impair T-cell-dependent antibody responses in mice lacking the actin-bundling protein L-plastin. *Eur J Immunol*. 2013;43(7): 1735-1744.
48. Unkel B, Hoegner K, Clausen BE, et al. Alveolar epithelial cells orchestrate DC function in murine viral pneumonia. *J Clin Invest*. 2012;122(10): 3652-3664.
49. Gutiérrez F, Masiá M, Mirete C, et al. The influence of age and gender on the population-based incidence of community-acquired pneumonia caused by different microbial pathogens. *J Infect*. 2006;53(3):166-174.
50. Ludwig E, Bonanni P, Rohde G, Sayiner A, Torres A. The remaining challenges of pneumococcal disease in adults. *Eur Respir Rev*. 2012;21(123):57-65.
51. Grau I, Ardanuy C, Calatayud L, Schulze MH, Liñares J, Pallares R. Smoking and alcohol abuse are the most preventable risk factors for invasive pneumonia and other pneumococcal infections. *Int J Infect Dis*. 2014;25:59-64.